Study of the microstructure effect of SPD-treated titanium on microhardness and corrosion resistance in physiological environments for implantology purposes

E.G. Zemtsova [1] ✉, A.A. Petrov [1], S.O. Kirichenko [1], N.F. Morozov [1],

V.K. Kudymov [2], A.Yu. Arbenin [1], B.N. Semenov [1], V.M. Smirnov [1]

[1] St. Petersburg State University, St. Petersburg, Russia

[2] St. Petersburg State University of Film and Television, St. Petersburg, Russia

✉ ezimtsova@yandex.ru

Abstract. Increasing the duration and quality of human life requires solving a number of medical and materials science problems, in particular, the creation of materials designed for long-term work in contact with the biological environment. When creating such materials for medical devices, it is necessary to take into account that they must meet strict requirements, namely, be biologically compatible with tissues, have corrosion resistance to various biological fluids and have increased wear resistance. The study of the effect of Ti microstructure on microhardness and its corrosion resistance in physiological environments is necessary to create implants designed for long-term work in contact with the biological environment of the body. In accordance with this, the purpose of this work was to establish the nature of the relationship between the structural properties of ultrafine-grained Ti with different sizes of crystallites (grains) obtained using equal-channel angular pressing (ECAP) of different intensity, namely with a different number of processing cycles, on the microhardness and stability of Ti in a corrosive environment.
Keywords: ultrafine-grained titanium; corrosion resistance; microhardness; intense plastic deformation; implants

Citation: Zemtsova EG, Petrov AA, Kirichenko SO, Morozov NF, Kudymov VK, Arbenin AY, Semenov BN, Smirnov VM. Study of the microstructure effect of SPD-treated titanium on microhardness and corrosion resistance in physiological environments for implantology purposes. *Materials Physics and Mechanics.* 2023;51(4): 1-10. DOI: 10.18149/MPM.5142023_1.

Introduction

Currently, titanium is widely used as a material for dental implants. This is explained by a number of physical and mechanical properties of both pure Ti and its alloys, such as: high elasticity modulus, tensile strength, fatigue strength combined with low cytotoxicity. At the same time, Ti, due to the presence of a natural 2-6 nm thick oxide layer, is passive to most existing corrosive media under standard (e.g. physiological) conditions. A number of studies [1,2] have shown how the thickness and protective properties of the oxide film

on the Ti surface depend on the external conditions of the physiological environment. Our research was aimed at identifying the relationship between the nano- and microstructure of Ti and its corrosion resistance in the physiological environments. Mechanical processing of metals makes it possible to obtain nanostructured Ti with a reduced crystallite size in order to enhance its physical and mechanical characteristics. In particular, severe plastic deformation (SPD) of Ti and its alloys is used for the production of ultrafine-grained titanium (UFG-Ti) with a tensile strength above 1000 MPa [3–6], which is significantly higher than the usual values of the tensile strength of coarse-grained (CG) Ti.

The main studies devoted to the corrosion stability of Ti with a reduced crystallite size were aimed at identifying the relationship between corrosion resistance in acidic media (HCl, H_2SO_4) and the microstructure of samples [7–9]. A number of studies are devoted to Ti corrosion in artificial physiological media (simulated body fluid) [10–12]. The conducted studies show that the corrosion resistance of UFG-Ti is explained by a combination of the effects of grain size reduction and the basic surface texture [11,13,14].

It is known that electrochemical corrosion of Ti in saliva-type physiological media can trigger allergic reactions [15], in addition, the presence of Ti ions can have a negative effect on the survivability and differentiation of osteoblasts [16], which certainly affects the feasibility and prospects of using dental implants. It is also known that prophylactic agents often contain fluorides in their composition, which lead to the destruction of the passivation film on the Ti surface and its further dissolution [17]. A comprehensive analysis of the mechanical and corrosion properties of UFG-Ti will expand the scope of application of this type of materials in implantology [18,19]. In accordance with this, the purpose of this work was to establish the nature of the relationship between the mechanical and structural properties of UFG-Ti with different sizes of crystallites (grains) obtained using Equal channel angular pressing (ECAP) of different intensity (with different number of processing cycles), and its resistance in a corrosive environment. As a corrosive medium, an environment was chosen that, in terms of salt composition and temperature regime, is close to physiological body fluids and at the same time enriched with fluoride ions. The results will contribute to the development of methods for synthesizing materials for implantology with specified mechanical and corrosion properties.

Experimental

Microhardness measurements. Square-shaped Ti samples were made from rods of commercially available Ti ASTM Grade 4 alloy of nominal composition (wt. %) Fe 0.10 %, Si 0.12 %, O 0.04 %, N 0.01 % H and 0.3 % other elements. The samples were subjected to severe plastic deformation (SPD) on an ECAP unit with a channel intersection angle of 105° at 400 °C. Depending on the number of repeated passage cycles in the ECAP channel, the samples are designated UFG 2, UFG 4, UFG 6, UFG 8, UFG 10, UFG 12, respectively. The sample designated "(CG) coarse grained" was used without deformation treatment as a reference.

Thick (3 mm) samples were cut transversely from the rods of the material on an electric erosion machine, filled with epoxy resin into the slice, and then their surface was mechanically polished on carbide-silicon sandpapers of grades 320, 600, 800, 1000 and 1200, and then sequentially polished on a Buehler Automet 250 grinding and polishing machine using polishing suspensions based on corundum and silicon oxide (5, 1 μm, 200 and 50 nm), respectively. At the end of the mechanical processing, the samples were extracted from the fillings, washed in an ultrasonic bath in isopropanol and deionized water and dried.

Transmission electron microscopy. TEM studies of the structures were performed on transmission electron microscopes JEM 2000EX and JMX200CX at accelerating voltages of

200 and 120 kV, respectively. Foils for electron microscopic studies were prepared by standard methods on a jet electropolishing device.

Measurement of microhardness. Microhardness was measured on a HMV-2T microhardometer manufactured by Shimadzu Corporation, which allows stepwise application of loads from 250 mN to 20 N. The Vickers method of the recovered print was used. The indenter was a regular four-sided diamond pyramid with an angle of 136° between opposite faces. The correctness of the microhardness determination was checked by reference samples with hardness 278 HV, 467 HV and 768 HV. Hereafter, the hardness is given in conventional HV units in accordance with the standards; the implied physical dimension is [kgs/mm^2]. For each material, 10 hardness determinations were carried out on 2 separate samples, the values were averaged, indentation was carried out near the geometric center of the grinds with the application of a load for 15 seconds.

Electrochemical measurements. All electrochemical measurements were carried out using a Solartron 1287 potentiostat/galvanostat with a Solartron 1260 impedance meter (Solartron Analytical) with native software. An original electrochemical cell was made according to the classical three-electrode scheme with a sponge Pt counter electrode, a AgCl electrode with a saturated KCl solution connected to the cell via a salt bridge (Luggin capillary) served as a reference electrode, a Ti sample was the working electrode. The potentiodynamic measurements were carried out with a standard sweep speed of 0.1667 mV/s. During measurements in the cell, the solution was maintained at 35 ± 0.5 °C using an external thermostat. 15 minutes before and during the measurement, the solution was stirred with a mechanical stirrer and bubbled with nitrogen (purity 99.999, 100 mL/min). A working solution of 0.15 M NaCl and 0.05 M NH$_4$F was prepared from chemically pure reagents using deionized water (25 MOhm·cm, Millipore Simplicity UV). 500 mL of the solution was used for each measurement. The pH was maintained at 7.2 with a pH electrode control on the Hanna Instruments meter.
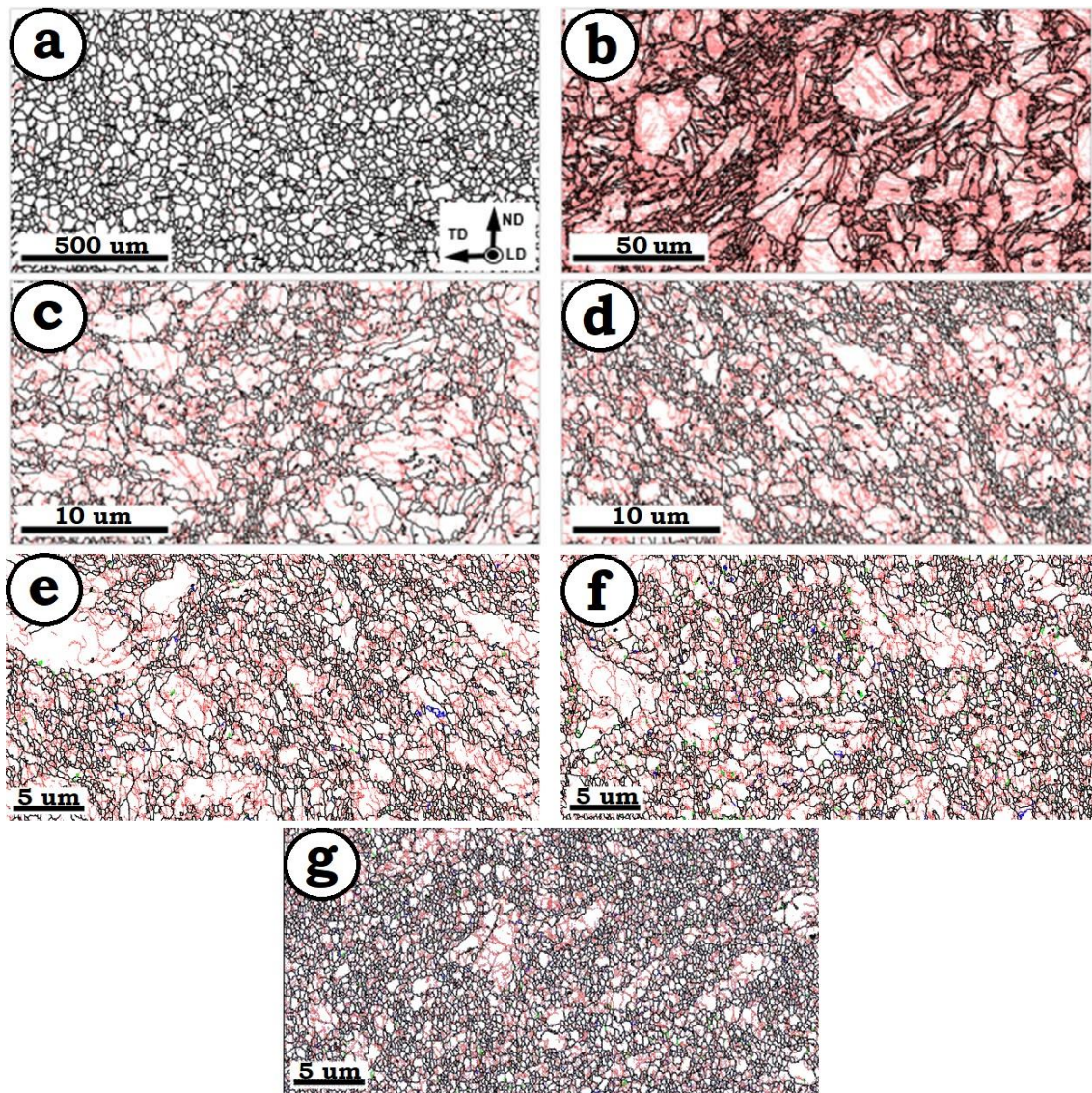
Results and Discussion

Microstructure of samples. To determine the microstructure of samples subjected to SPD, their high-resolution EBSD maps were obtained, fragments of which are shown in Fig. 1. These maps show a complex grain structure, grain size and grain boundaries in Ti samples: small-angle (SA), large-angle (LA), as well as double grain misorientation.

Already after the first two ECAP cycles (sample UFG 2), the transformation of the initial titanium grains led to a microstructure complication (Fig. 1(b)). In Russian publications, it is also known as fragmentation [9]. During the further increase of accumulated deformation, intensive formation of equiaxed grains of submicrocrystalline size took place in the structure of UFG 4 and UFG 6 samples (Fig. 1(b,c)). Note also the almost complete disappearance of the twin boundaries from the microstructure (Fig. 1(c)) as the deformation increases.

A further increase in deformation in UFG 8 - UFG 12 samples did not lead to significant changes in the microstructure morphology, but only contributed to a gradual increase in the small grains fraction (Fig. 1(g)).

Figure 2 shows the dependences of the density of small-angle and large-angle grain boundaries, as well as the total density of the boundaries on the number of ECAP cycles. It is possible to note an increase in the proportion of large-angle grain boundaries as a result of SPD after 1-12 cycles of ECAP and a decrease in the proportion of small-angle grain boundaries after 8 cycles of ECAP.

4 E.G. Zemtsova, A.A. Petrov, S.O. Kirichenko, N.F. Morozov, V.K. Kudymov, A.Yu. Arbenin, B.N. Semenov,
V.M. Smirnov

Fig. 1. Fragments of high-resolution EBSD maps of the material after various ECAP
stages: coarse grained (CG) (a), 2 cycles (b), 4 cycles (c), 6 cycles (d), 8 cycles (e),
10 cycles (f), 12 cycles (g). On the SD cards SA, LA, and disorientation 85° <2110> and
74° <2110> are indicated by red, black, blue and green lines, respectively
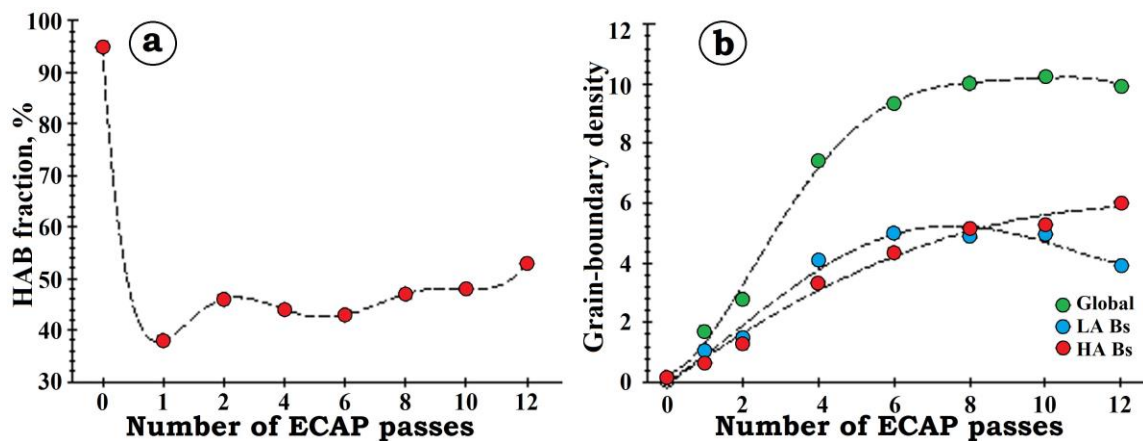
Fig. 2. Dependences of grain boundary density (a) and the proportion of large-angle
boundaries (b) on the number of ECAP cycles

The crystallite sizes in the samples measured using the scattered electrons diffraction are shown in Table 1. These values indicate that SPD of Ti samples led to a significant decrease in the grain size.

**Table 1.** Average size of CG-Ti crystallites and SPD-subjected Ti samples

Sample	Size of crystallites, µm
CG-Ti	30-60
UFG-Ti 2	5.0-10.0
UFG-Ti 4	1.0
UFG-Ti 6	0.5-1.0
UFG-Ti 8	0.4-0.6
UFG-Ti 10	0.2-0.3
UFG-Ti 12	0.2

Microhardness measurements. When measuring hardness using the Vickers method, a well-known difficulty is the dimensional effect – the dependence of the measured hardness on the magnitude of the applied load or the depth of indenter insertion (indentation size effect). Therefore, to determine the load boundary at which this effect influences the results, microhardness was measured on the samples of CG and UFG-Ti 10 at loads 0.01, 0.025, 0.05, 0.1, 0.2, 0.3, 0.5, 1 and 2 HV (98.07, 245.20, 490.30, 980.70 mN, 1.960, 2.942, 4.903, 9.807 and 19.614 N, respectively), see Fig. 3.

The resulting hardness values become almost constant at loads above 0.3 HV (Fig. 3). As a result, we selected a load of 0.3 HV as the operating value. The obtained microhardness data of the samples are shown in Fig. 4.
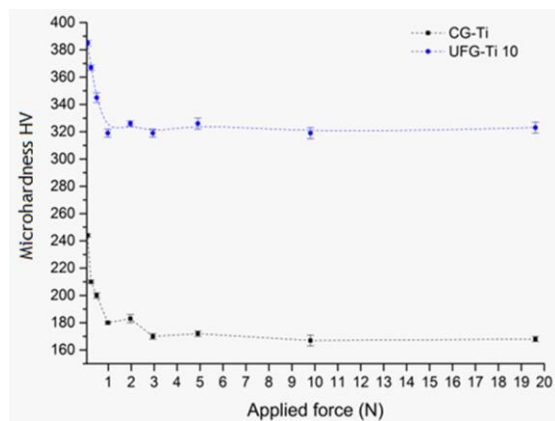
Fig. 3. Dependence of microhardness (at 15-second exposure) on the applied load for the CG-Ti comparison sample and for UFG-Ti 10 sample subjected to 10 cycles of ECAP
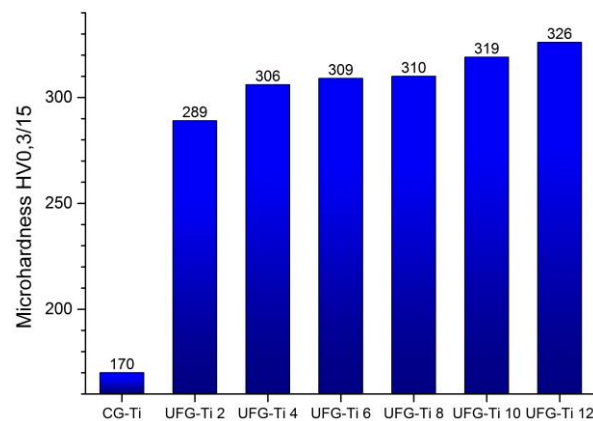
Fig. 4. Change in the microhardness measured at a load of 0.3 N for 15 seconds for Ti, depending on the ECAP cycles number

It can be seen that, in general, UFG-Ti samples exceed CG-Ti samples in microhardness by more than 1.5 times, while the microhardness dependence on the number of SPD treatments is much weaker.

Apparently, the increased hardness of UFG-Ti is mainly a consequence of a grain size decrease. The grain size decrease, in turn, is associated with high shear deformations that occurred in the material during processing. According to ECAP along the BC route, Ti samples were subjected to SPD when passing through the matrix from 2 to 12 times. Estimating the Vickers microhardness values, we can conclude that the main increase in the mechanical properties of Ti is achieved already at the first 2–4 passes. Compared with Ti of

the initial grain size, the microhardness increases by more than 1.5 times. During further processing, no significant changes in microhardness are observed: 12 passes increased the hardness by only 6.5 % relative to the sample subjected to 4 passes.

Corrosion measurements. The difference in the corrosion behavior with a decrease in the size of Ti crystallites is demonstrated by measurements of the linear polarization resistance (Fig. 5).
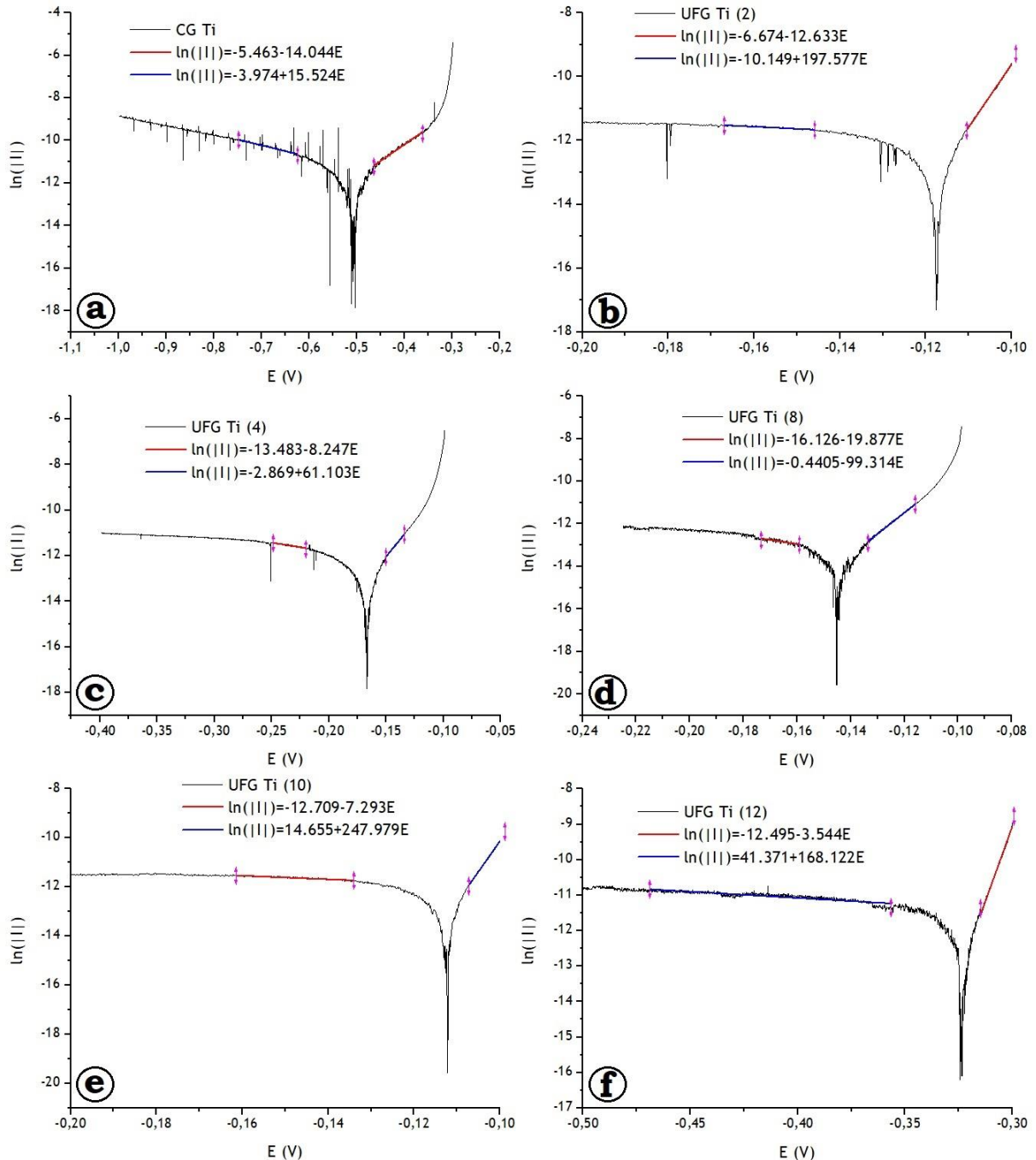
**Fig. 5.** Polarization curves of Ti subjected to SPD treatment

By approximating the linear sections of the polarization curves of Ti samples, the values of current and corrosion potential were obtained. The data are presented as dependencies on the number of passes through the ECAP device in Fig. 6.
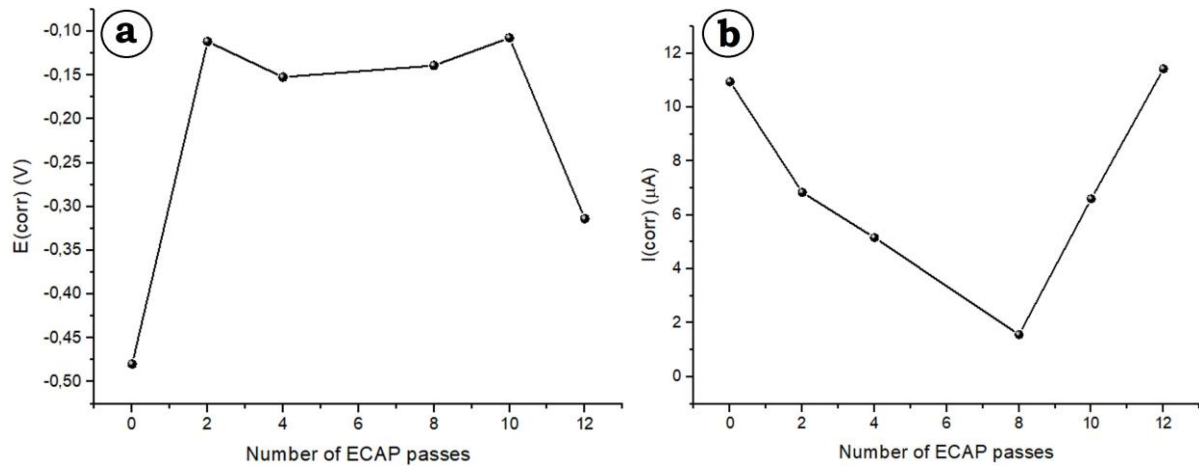
Fig. 6. Dependences of the potential (on the left) and the corrosion current of Ti on the number of ECAP cycles

Note the non-monotonic nature of the dependencies, which manifests itself in an increase in the corrosion resistance of titanium samples in the range from 0 to 8 cycles, followed by its decrease. This is expressed in the potential increase and the current decrease at the start of the dependence, followed by a potential decrease and the corrosion current increase. At the same time, if the dependence of the Ti corrosion current on the number of ECAP cycles has a pronounced minimum at 8 cycles, then the corrosion potential dependence has a plateau area between from 2 and 10.

Taking into account the extremely high values of Tafel slopes at the anode site and anode exchange currents (Fig. 5), it can be assumed that the corrosion current is most limited by the depolarization process speed (reduction of components of the corrosive medium on the corroding metal surface). This can be verified by comparing the dependence in Figure 6 with the dependences of the Tafel slope of the cathode section and the cathode exchange current on the number of ECAP cycles (Fig. 7).
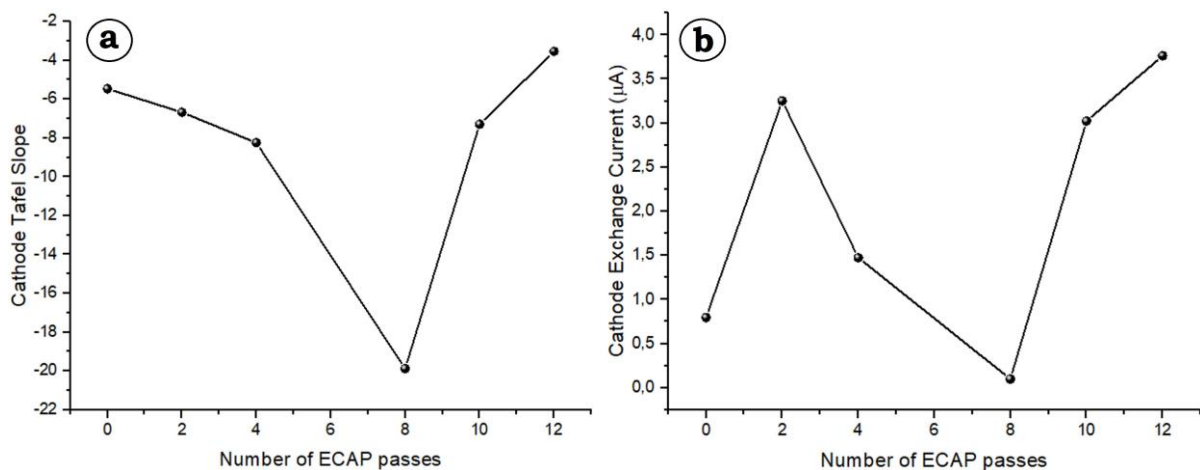
Fig. 7. Dependence of the Tafel slope of the cathode section (a) and the cathode exchange current (b) on the number of ECAP cycles

Despite the fact that the dependence of the absolute value of the Tafel slope of the cathode section has a maximum in the same region in which the minimum dependence of the corrosion current is detected, the presence of a minimum exchange current leads to the formation of a minimum corrosion current in this region.

Thus, it can be confidently assumed that the factor largely determining the corrosion rate of ECAP-subjected Ti is the cathodic exchange current. This means, that the process speed is limited by the depolarization. This may be due to the depassivation of the TiO_2 film when interacting with a medium containing fluoride ions, in relation to the semi-reaction of Ti oxidation. At the same time, the preservation of the oxide film leads to difficulties in the process of electron transfer through the electrode-electrolyte surface, as a result of which the depolarization reaction becomes limiting.

At the same time, the depolarization rate can be limited not only by the oxide film thickness, but also by the degree of saturation of the Ti (electrode) surface with hydrogen, including also the areas of grain boundaries reaching the surface. This statement is true for all samples, regardless of the number of ECAP cycles.

Based on these statements, the following explanation of the observed dependencies can be put forward. As follows from the EBSD data (Fig. 2), the use of 2 to 8 ECAP cycles leads to an increase in the density of large-angle grain boundaries in the Ti bulk. The increase in corrosion resistance may occur due to the disordering of the surface of the sample slice in the area of the existence of the LA, in particular, as a result of hydrogen saturation of the grain interface. With an increase in the proportion of areas of the LA output to the electrode (Ti) surface, the degree of hydrogen saturation of the metal surface increases due to the increased rate of hydrogen diffusion in disordered regions. In addition, the influence of the preferential orientation of crystallites is possible, but the discussion of this effect requires more experiments. With further (> 8 cycles) ECAP of Ti, the factor of reducing the grain size and the proportion of grain boundaries begins to play an important role. The subsequent changes in the texture of the slice and an increase in the reaction surface area of the grains, as well as the disordering of the oxide film, lead to an increase in the corrosion current, which leads to a sharp drop in the corrosion resistance of Ti.

Conclusion

Thus, this paper demonstrates the relationship between the microstructure, mechanical properties and corrosion resistance of Ti samples subjected to equal-channel angular pressing (ECAP).

The microhardness data of the samples demonstrate an increase in the hardness of fine-grained titanium due to a decrease in the grain size in the Ti bulk. Analysing the Vickers microhardness values, we can conclude that the main increase in the mechanical properties of Ti (more than 90 %) is achieved already after the first 2-4 cycles of ECAP processing. Compared with the initial Ti, the microhardness of SPD-treated Ti samples increases by more than 1.5 times.

It was shown that the electrochemically determined corrosion resistance of Ti subjected to ECAP, varies non-linearly depending on the structure of Ti. The non-monotonic nature of the dependencies, which manifests itself in an increase in the corrosion resistance of titanium samples in the interval from 2 to 8 cycles, followed by its decrease, may occur due to the disordering of the surface of the sample section in the region of the existence of the proportion of large-angle grain boundaries in the volume of titanium, in particular, as a result of the With further Ti ECAP, more than 8 cycles, a significant role in the corrosion resistance of titanium begins to be played by the factor of reducing the grain size in the bulk sample and, as a consequence, an increase in the reaction surface area of the grains, which leads to a sharp drop in the Ti corrosion resistance. Therefore, to create Ti implants with improved strength characteristics and at the same time resistant to corrosion in physiological body fluids, it is necessary to use Ti blanks subjected to 4 to 8 ECAP cycles.

References
1. Mathew MT, Abbey S, Hallab NJ, Hall DJ, Sukotjo C, Wimmer MA. Influence of pH on the tribocorrosion behavior of CpTi in the oral environment: synergistic interactions of wear and corrosion. *J. Biomed. Mater. Res. Part B*. 2012;100B(6): 1662–1671.
2. Li J, Li SJ, Hao YL, Huang HH, Bai Y, Hao YQ, Guo Z, Xue JQ, Yang R. Electrochemical and surface analyses of nanostructured Ti–24Nb–4Zr–8Sn alloys in simulated body solution. *Acta Biomater*. 2014;10(6): 2866–2875.
3. Stolyarov VV, Zhu YT, Lowe TC, Islamgaliev RK, Valiev RZ. A two-step SPD processing of ultrafine-grained titanium. *Nanostruct. Mater*. 1999;11(7): 947–954.
4. Stolyarov VV, Zeipper L, Mingler B, Zehetbauer M. Influence of post-deformation on CP-Ti processed by equal channel angular pressing. *Mater. Sci. Eng. A*. 2008;476(1-2): 98–105.
5. Sabirov I, Perez-Prado MT, Molina-Aldareguia JM, Semenova IP, Salimgareeva GK, Valiev RZ. Anisotropy of mechanical properties in high-strength ultra-fine grained pure Ti processed via a complex severe plastic deformation route. *Scripta Mater*. 2011;64(1): 69–72.
6. Zhao X, Fu W, Yang X, Langdon TG. Microstructure and properties of pure titanium processed by equal-channel angular pressing at room temperature. *Scripta Mater*. 2008;59(5): 542–545.
7. Wang ZB, Hu HX, Zheng YG. Determination and explanation of the pH-related critical fluoride concentration of pure titanium in acidic solutions using electrochemical methods. *Electrochim. Acta*. 2015;170: 300–310.
8. Balyanov A, Kutnyakova J, Amirkhanova NA, Stolyarov VV, Valiev RZ, Liao XZ, Zhao YH, Jiang YB, Xu HF, Lowe TC, Zhu YT. Corrosion resistance of ultra fine-grained Ti. *Scripta Mater*. 2004;51(3): 225–229.
9. Wanga ZB, Hua HX, Zhenga YG, Kea W, Qiaob YX. Comparison of the corrosion behavior of pure titanium and its alloysin fluoride-containing sulfuric acid. *Corrosion Science*. 2016;103: 50–65.
10. Balakrishnan A, Lee BC, Kim TN, Panigrah BB. Corrosion Behaviour of Ultra Fine Grained Titanium in Simulated Body Fluid for Implant Application. *Trends Biomater. Artif. Organs*. 2008;21(1): 58–64.
11. Gurao NP, Manivasagam G, Govindaraj P, Asokamani R, Suwas S. Effect of texture and grain size on bio-corrosion response of ultrafine-grained titanium. *Met. Mater. Trans.* 2013;44A: 5604–5610.
12. Rosalbino F, Delsante S, Borzone G, Scavino G. Influence of noble metalsalloying additions on the corrosion behaviour of titanium in a fluoride-containing environment. *J. Mater. Sci.-Mater. Med.* 2012;23: 1129–1137.
13. Hoseini M, Shahryari A, Omanovic S, Szpunar JA. Comparative effect of grain size and texture on the corrosion behaviour of commercially pure titanium processed by equal channel angular pressing. *Corros. Sci*. 2009;51(12): 3064–3067.
14. Wang ZB, Hu HX, Liu CB, Zheng YG. The effect of fluoride ions on the corrosion behavior of pure titanium in 0.05 M sulfuric acid. *Electrochim. Acta*. 2014;135: 526–535.
15. Sicilia A, Cuesta S, Coma G, Arregui I, Guisasola C, Ruiz E, Maestro A. Titanium allergy in dental implant patients: a clinical study on 1500 consecutive patients. *Clin. Oral. Implants. Res*. 2008;19(8): 823–835.
16. Mine Y, Makihira S, Nikawa H, Murata H, Hosokawa R, Hiyama A, Mimura S. Impact of titanium ions on osteoblast-, osteoclast- and gingival epithelial-like cells. *J. Prosthodont. Res.* 2010;54(1): 1–6.
17. Mabilleau G, Bourdon S, Joly-Guillou ML, Filmon R, Baslé MF, Chappard D. Influence of fluoride, hydrogen peroxide and lactic acid on the corrosion resistance of commercially pure titanium. *Acta Biomater*. 2006;2(1): 121–129.

18. Nazarov DV, Zemtsova EG, Solokhin A, Valiev RZ, Smirnov VM. Enhanced Osseointegrative Properties of Ultra-Fine-Grained Titanium Implants Modified by Chemical Etching and Atomic Layer Deposition. *ACS Biomaterials Science and Engineering*. 2018;4(9): 3268–3281.

19. Zemtsova EG, Morozov NF, Semenov BN, Valiev RZ, Smirnov VM. Mechanical properties of nanostructured titanium with bioactive titanium-organic nanocoating. *Materials Physics and Mechanics*. 2017;32(3); 253–257.

THE AUTHORS

Zemtsova E.G.
e-mail: ezimtsova@yandex.ru

Petrov A.A
e-mail: st068921@student.spbu.ru

Kirichenko S.O.
e-mail: sergkirichenko@gmail.com

Morozov N.F.
e-mail: n.morozov@spbu.ru

Kudymov V. K.
e-mail: v.k.kudymov@gmail.com

Arbenin A.Yu.
e-mail: aua47@yandex.ru

Semenov B.N.
e-mail: b.semenov@spbu.ru

Smirnov V.M.
e-mail: vms11@yandex.ru